Mechanisms of Development 123 (2006) 312–320

www.elsevier.com/locate/modo

# Homeotic transformations of the axial skeleton of *YY1* mutant mice and genetic interaction with the Polycomb group gene *Ring1/Ring1A*

Mar Lorente [a,1], Claudia Pérez [b], Carmen Sánchez [a], Mary Donohoe [c,2], Yang Shi [c], Miguel Vidal [a,*]

[a] *Developmental and Cell Biology, Centro de Investigaciones Biológicas, CSIC, Ramiro de Maeztu 9, 28040 Madrid, Spain*
[b] *Anatomy and Histopathology, Facultad de Veterinaria, Universidad de León, Campus Vegazana, 24071 León, Spain*
[c] *Deparment of Pathology, Harvard Medical School, 77 Avenue Louis Pasteur, Boston, MA 02115, USA*

Received 26 July 2005; received in revised form 10 February 2006; accepted 24 February 2006
Available online 18 April 2006

**Abstract**

Polycomb group (PcG) proteins participate in the maintenance of transcriptionally repressed state of genes relevant to cell differentiation. Here, we show anterior homeotic transformations of the axial skeleton of $YY1^{+/-}$ mice. We find that the penetrance of some of these alterations was reduced in mice that are deficient in the class II PcG gene *Ring1/Ring1A*, indicating a genetic interaction between those two genes. Further support for this interaction is an abnormal anterior eye formation in *Ring1*-deficient mice, which is enhanced in compound $YY1^{+/-}Ring1^{-/-}$ mice. In addition, YY1 forms complexes with Ring1 and other class II PcG proteins such as Rnf2 and Bmi1 in GST pull down experiments in transfected cells. These findings provide evidence for a PcG function for YY1 in vertebrates.


*Keywords:* Polycomb group genes; YY1; Ring1; Axial skeleton; Anterior eye

## 1. Introduction

Maintenance of transcription patterns of key regulatory genes is needed throughout development and lifetime of organisms. This requirement is satisfied in part by the functions of the Polycomb group (PcG) and trithorax group (trxG) of proteins, maintaining repressed and active gene expression patterns, respectively [see (Ringrose and Paro, 2004; Brock and Fisher, 2005) for recent reviews]. The PcG genes were first identified in *Drosophila* as negative regulators of homeotic genes. Functional and structural homologs have been subsequently identified in worms, vertebrates and plants. In vertebrates, the PcG proteins play a role not only in the specification of the antero-posterior axis but also in X chromosome silencing, genomic imprinting, stem cell renewal, or cell differentiation (Lessard and Sauvageau, 2003; Valk-Lingbeek et al., 2004).

The PcG proteins belong to a variety of complexes (Otte and Kwaks, 2003). Those in which PcG polypeptides account for most of their components can be categorized by the mutually exclusive presence of either a histone H3 methyl transferase activity (class I PcG complexes) or a E3 ubiquitin ligase activity (class II PcG complexes). The core members of the class I complexes include the products of the embryonic endoderm development (EED) gene, and the enhancer of zeste homologs (EZH) which are histone H3K27 methyltransferases (Cao et al., 2002; Czermin et al., 2002; Kuzmichev et al., 2002; Muller et al., 2002). The core members of the class II complexes include the products of the paralogs of *Polycomb*, *Polyhomeotic*, *Posterior sex combs genes*, and the E3 ubiquitin ligase encoded by the *Sex combs extra/Rnf2* (*Ring1*B) gene (Wang et al., 2004b). A subset of class II PcG proteins are also found as minor components of other histone methyl tranferases-containing complexes (Ogawa et al., 2002; Shi et al., 2003).

PcG-mediated gene repression can take place through several mechanisms that include chromatin structure and interference with the activities of RNApolII or chromatin remodeller complexes. (Levine et al., 2004; Pirrotta and Gross,

* Corresponding author. Tel.: +34 91 837 3112; fax: +34 91 536 0432.
*E-mail address:* mvidal@cib.csic.es (M. Vidal).
[1] Present address: Biochemistry and Molecular Biology I, Facultad de Biología, Universidad Complutense, Av. Complutense s/n, 28040 Madrid, Spain.
[2] Present address: Department of Molecular Biology, Massachusetts General Hospital and Department of Genetics, Harvard Medical School, Boston, MA 02114, USA.

0925-4773/$ - see front matter © 2006 Elsevier Ireland Ltd. All rights reserved.
doi:10.1016/j.mod.2006.02.003

2005). PcG proteins associate to DNA sequences known as Polycomb response elements (PREs) so far only identified in *Drosophila* (Ringrose et al., 2003). These PREs contain consensus sites for a number of DNA binding proteins that are thought to target PcG proteins to PREs (Horard et al., 2000; Americo et al., 2002; Dejardin et al., 2005). Among these are the Krüppel-like zinc finger proteins pleiohomeotic (pho) and pleiohomeotic-like (phol), the only PcG proteins that are able to bind in purified form to DNA (Brown et al., 1998, 2003). Pho and phol are homologs of the ubiquitous mammalian transcription factor Yin Yang 1 (YY1). The conserved sequences include a 22 amino acids box, and a C-terminal DNA binding domains made of four zinc-fingers.

In selected DNA targets, YY1/pho/phol participate in the recruitment of class I PcG complexes and the modification of nucleosomes by H3K27 methylation (Caretti et al., 2004; Srinivasan and Atchison, 2004; Wang et al., 2004a). Subsequently, chromodomain-containing class II PcG complexes are recruited, possibly by docking to the methylated nucleosomes. YY1 interacts directly with EED/esc (Satijn et al., 2001), and with EZH1 (Wang et al., 2004a). Despite these activities, neither YY1 nor its fly homologs have been found as part of the isolated PcG complexes. Evidence of a PcG function for vertebrate YY1 proteins comes mostly from its ability to (partially) rescue the phenotype of pho mutant flies (Atchison et al., 2003). In *Xenopus* embryos, the downregulation of YY1 affects antero-posterior neural patterning (Kwon and Chung, 2003). In the mouse, the genetic analysis is hampered by the early lethality of *YY1* deficient embryos, which degenerate around the time of implantation (Donohoe et al., 1999).

Here, we investigated a *YY1* loss-of-function mouse mutant line in search for evidence for a PcG related phenotype. We found homeotic transformations and other alterations of the axial skeleton in $YY1^{+/-}$ mice. In addition, we obtained evidence for a genetic interaction between *YY1* and the *Ring1*/*Ring1A*, a class II PcG gene.

## 2. Results

### 2.1. Axial skeleton of $YY1^{+/-}$ mice

Mice deficient in PcG products usually show axial skeleton alterations of which some can be interpreted as homeotic transformations. Even though these malformations are normally seen only in homozygous mutant mice, there are exceptions such as the *Ring1* mutant mice (del Mar Lorente et al., 2000), which prompted us to examined the axial skeletons of $YY1^{+/-}$ mice. Newborn offspring from interbred $YY1^{+/-}$ mice showed frequent alterations in the thoracic and lumbo-sacral regions of the axial skeleton as summarised in Table 1. The thoracic region of wild type mice spans vertebrae 8–20 (corresponding to thoracic vertebrae 1–13), and characteristically have ribs. Of these, the first seven are called vertebrosternal because they are attached both to thoracic vertebrae T1–T7 and to the sternum (Fig. 1A). Some $YY1^{+/-}$ mice, however, showed eight vertebrosternal ribs because the rib attached to the thoracic vertebra 8 (T8) was also attached to the sternum (Fig. 1B). This malformation corresponds to a transformation of the identity of the vertebrae T8 in that of vertebra T7. In the lumbar region, located between the thirteen rib-bearing thoracic vertebrae and the more frontal sacral vertebrae, about 40% of $YY1^{+/-}$ mice showed uni- or bi-lateral cartilaginous condensations (rudimentary ribs) attached to the 21st vertebra (Fig. 1F), which in wild type mice (Fig. 1E) is the first lumbar vertebra (L1). This alteration is described as a L1–T13 transformation. A very common alteration (70% of mice) was the change of the position of the so-called transitional vertebra. This vertebra marks a change in orientation of the posterior process, which points posteriorly in vertebrae T3–T9 and anteriorly in vertebrae T11 and other more caudal. In wild type mice the 17th vertebra or thoracic 10 (T10), is the transitional vertebra (Fig. 1C), whereas in $YY1^{+/-}$ mice (Fig. 1D) it has the appearance of the thoracic vertebra T9 (T9). Finally, the most frequent alteration seen in $YY1^{+/-}$ mice was the abnormal localization of sacro-iliac joints at the 28th vertebrae (Fig. 1F,G), which corresponds to the second lumbar vertebra (S2) whereas in wild type mice (Fig. 1E) it occurs through the first sacral vertebra (S1). In summary, $YY1^{+/-}$ mice showed, with variable penetrance, a number of skeletal alterations, which can be interpreted as anterior homeotic transformations.

It is thought that the skeletal alterations observed in PcG mutant mice are due to the deregulation of Hox gene expression. We studied the expression patterns of a number of Hox genes by whole mount in situ hybridization to 11.5 dpc embryos. These included Hoxc6, Hoxc8 and Hoxc9, which mark the anterior, middle and posterior thoracic domains, respectively, and Hoxd11, which marks the sacral region.

Table 1
Skeletal alterations in $YY1^{+/-}$ mice and in compound *YY1*, *Ring1* mutant mice

| | Wild type $n=16$ | $YY1^{+/-}$ $n=15$ | $Ring1^{+/-}$ $n=10$ | $Ring1^{-/-}$ $n=20$ | $YY1^{+/-}Ring1^{+/-}$ $n=9$ | $YY1^{+/-}Ring1^{-/-}$ $n=11$ |
|---|---|---|---|---|---|---|
| C2–C1 | 0 | 0 | 4 (40) | 5 (40) | 2 (22) | 3 (27) |
| Abnormal C2 | 1 (6) | 1 (7) | 1 (10) | 6 (30) | 3 (33) | 0 |
| T8–T7 | 1 (6) | 4 (27) | 1 (10) | 6 (30) | 3 (33) | 4 (36) |
| T10–T9 | 0 | 11 (73) | 0 | 0 | 3 (33) | 4 (36) |
| L1–T13 | 1 (6) | 6 (40)[a] | 2 (20) | 5 (40) | 4 (44) | 5 (45) |
| S2–S1 | 0 | 13 (87)[a] | 0 | 0 | 3 (33) | 8 (73) |

C1, atlas; C2, axis; T7, T8, T9, T10, T13, 7th, 8th, 9th, 10th, 13th thoracic vertebae; L1, 1st lumbar vertebra. S1, S2, 1st, 22nd sacral vertebrae. Penetrance of the skeletal abnormalities is indicated (between brackets) as percentage of mice analyzed.

[a] Unilateral and bilateral abnormalities were scored as positive in the analysis.

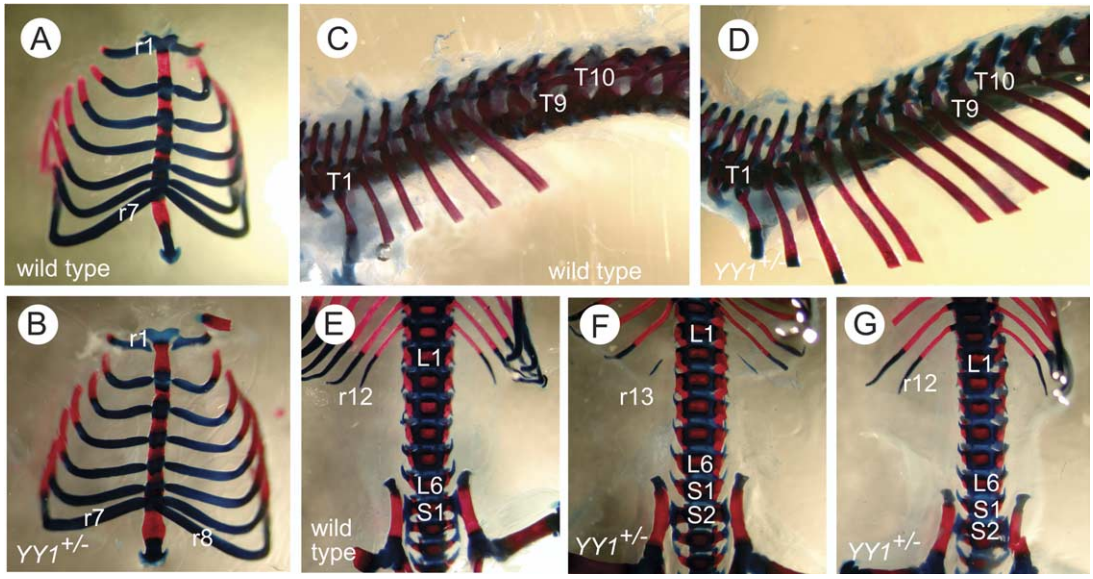


Fig. 1. Skeletal alterations of newborn *YY1*$^{+/-}$ mice. Views of the thoracic (A,D) and lumbar (E,G) regions of cleared skeletons of wild type (A,C,E) and *YY1* heterozygous (B,D,F,G) mice. Cartilage and bone appear in blue and red after staining with a mixture of Alcian Blue and Alizarin Red, respectively. (A,B) Anterior transformation of the eight thoracic (T8) vertebra. Ventral view of the thorax of wild type (A) and mutant mice showing the rib attached to T8 joined to the sternum (B). (C,D) Anterior transformation of the 10th thoracic (T10). Side view of the midthoracic region. The transitional vertebra, which is normally observed in T10, had the appearance of the 9th thoracic (T9) vertebra in mutant mice. (E,F) Anterior transformation of the first lumbar (L1) vertebra in the 13th thoracic (T13) vertebra. Dorsal view of the lumbar region of a wild type (E) and a mutant mice (F) showing ectopic condensations of cartilage (rudimentary rib r14) on both sides of the first lumbar (L1) vertebra. (F,G) Anterior transformation of the second sacral (S2) vertebra in the first sacral (S1) vertebra. Ventral views of mice from the posterior thoracic to the anterior sacral region. In wild type mice (E) the first sacral vertebra (S1) is fused with the transverse processes to form sacral bone, whereas in the mutant mice (F,G) it is the second sacral vertebra (S2). In dorsal and ventral views, anterior is top. In lateral views, anterior is to the left. L6 is the sixth lumbar vertebra. (For interpretation of the references to colour in this figure legend, the reader is referred to the web version of this article.)

However, we observed no differences between the expression patterns of these genes in *YY1*$^{+/-}$ and wild type littermates embryos (data not shown). We extended the analysis to other Hox genes, such as Hoxa3, Hoxa4, Hoxb4, Hoxd4, and Hoxb8, but their expression patterns were not affected (data not shown). Because transient alterations of Hox gene expression have been associated to axial skeleton phenotypes (Zakany et al., 1997; Juan and Ruddle, 2003) we also analyzed the expression of these Hox genes in 8.5 dpc *YY1*$^{+/-}$ embryos but found no differences with that seen in wild type littermates (data not shown).

We then used an alternative model of early differentiation to look into Hox gene regulation by YY1. Since YY1 null blastocysts are not viable (Donohoe et al., 1999) *YY1*$^{+/-}$ and wild type ES cells were derived from littermates blastocysts and Hoxb1, Hoxb3 and Hoxa4 gene expression analyzed during their differentiation into embryoid bodies (Fig. 2). The results showed a clear upregulation of Hoxb1 at day 6 of differentiation (Hoxb3 and Hoxa4 showed no expression)

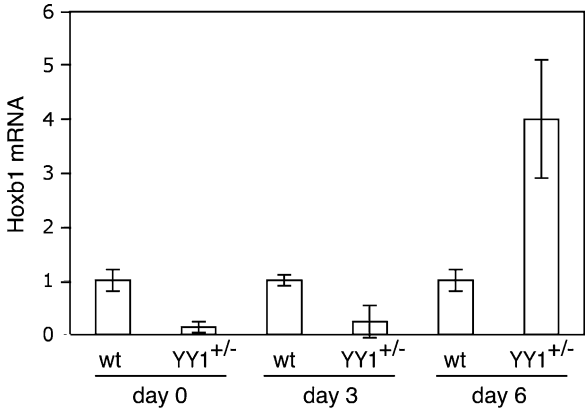


Fig. 2. Hox gene expression in differentiated *YY1*$^{+/-}$ ES cells. Hoxb1 mRNA was measured by quantitative RT-PCR during the indicated days of differentiation of wild type and *YY1*$^{+/-}$ ES cells to embryoid bodies. Hoxb1 mRNA levels are expressed after normalization to b-actin mRNA. Bars are standard deviation of average from triplicate determinations.

Table 2
Anterior eye defects

| | Wild type | YY1$^{+/-}$ | Ring1$^{-/-}$ | YY1$^{+/-}$-Ring1$^{-/-}$ |
|---|---|---|---|---|
| *New born mice* | *n*=6 | *n*=4 | *n*=13 | *n*=10 |
| Abnormal lens | 0 | 0 | 4 (30) | 6 (60) |
| Corneolenticular adhesion | 0 | 0 | 3 (24) | 7 (70) |
| *17.5 dpc embryos* | *n*=9 | *n*=4 | *n*=5 | *n*=10 |
| Abnormal lens | 0 | 0 | 2 (40) | 7 (70) |
| Corneolenticular adhesion | 0 | 0 | 2 (40) | 8 (80) |
| Hyperplasic lens epithelia | 0 | 0 | 3 (60) | 5 (50) |
| *15.5 dpc embryos* | *n*=2 | | *n*=9 | *n*=5 |
| Abnormal lens | 0 | n.d. | 3 (33) | 3 (60) |
| Corneolenticular adhesion | 0 | n.d. | 3(33) | 4(80) |

n.d., not done. Penetrance of alterations is indicated (between brackets) as percentage of mice analyzed.

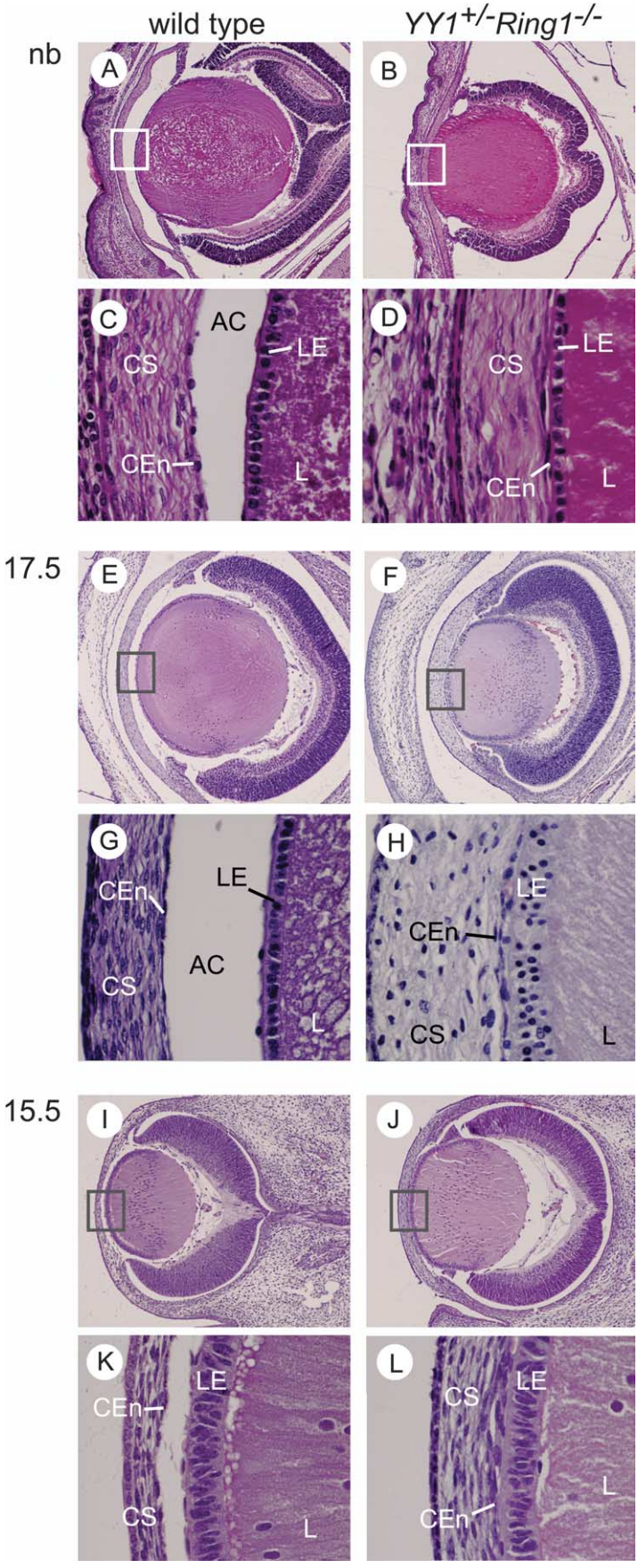
wild type
YY1+/-Ring1-/-
nb
A
B
C
AC
LE
CS
CEn
L
D
17.5
E
F
G
H
15.5
I
J
K
L

indicating that at least a subset of Hox genes are regulated by YY1.

### 2.2. Axial skeleton of compound YY1, Ring1 mutant mice.

Because of the homeotic transformations seen in *YY1*$^{+/-}$ mice we wished to investigate whether there is a genetic interaction between *YY1* and a PcG gene. We chose the class II PcG gene *Ring1*, which also show anterior homeotic transformations. Table 1 summarises the skeletal alterations observed in single mutant and compound *YY1*$^{+/-}$ *Ring1*$^{-/-}$ mice. The alterations of *Ring1* mutant mice were similar to those previously described (del Mar Lorente et al., 2000). These included the transformations of vertebra T8 into a T7 and that of vertebra L1 into a T13, both of which were also found in *YY1*$^{+/-}$ mice. The penetrance of these transformations was hardly affected in *YY1*$^{+/-}$ *Ring1*$^{-/-}$ mice. Likewise the alterations in the sacral region of *YY1*$^{+/-}$ were not much affected in the compound mutants. In contrast, the penetrance of the mislocalization of the transitional vertebra (transformation T10 into T9) seen in *YY1*$^{+/-}$ mice, and that of alterations in the cervical region of *Ring1* mice, were clearly reduced in the *YY1*$^{+/-}$ *Ring1*$^{-/-}$ mice. In summary, the penetrance of a subset of alterations differed in the compound mutants in comparison with that seen in single mutants. This is an indication of a genetic interaction between the *YY1* and *Ring1* genes.

### 2.3. Anterior eye development

Additional evidence for a genetic interaction between the *YY1* and *Ring1* genes was obtained from the histological examination of single and compound mutant mice. We found alterations in structures of the anterior segment of the eye. The results are summarised in Table 2. About 30% of newborn *Ring1*-deficient mice showed unilateral or bilateral abnormally shaped lens, in contact with the cornea, therefore lacking an anterior chamber (Fig. 3A–D). In wild type mice, this chamber forms during the differentiation of the corneal endothelium, when the lens detaches from the future cornea leaving a fluid-filled cavity. *YY1*$^{+/-}$ *Ring1*$^{-/-}$ mice showed similar alterations, although the penetrance of the defect was higher, and affected 60–70% of the mice. *YY1*$^{+/-}$ mice, on the other hand, were indistinguishable from the wild type. To see whether the synergistic effect of the combination of *YY1* and *Ring1* mutations on the anterior eye phenotype also occurred at earlier developmental stages we studied 17.5 and 15.5 dpc embryos. At 17.5 dpc (Fig. 3E,H), some of the *Ring1*-deficient embryos (40%) showed modified lenses and also lacked an anterior eye chamber. Often, these embryos showed unilaterally a hyperplastic, multilayered, lens epithelium, in contrast with the one-layer epithelium seen in wild type embryos (Fig. 3G,H). In addition, the mesenchymal cells of the presumptive cornea were less compacted and were surrounded by more extracellular matrix than those in wild type littermates (Fig. 3H). Whereas this phenotype was not affected by a reduction in the dosage of *YY1*, the penetrance of the corneolenticular adhesion was enhanced, appearing in 80% of *YY1*$^{+/-}$ *Ring1*$^{-/-}$ mice. Interestingly, the lens epithelium defect observed in 17.5 dpc embryos is a transient alteration, which was observed neither earlier at 15.5 dpc (Fig. 3K,L) nor in newborn mice (Fig. 3C,D). At the earliest stage examined, 15.5 dpc (Fig. 3I,L), one third of the *Ring1*-deficient embryos lacked an anterior eye chamber, and as in later stages, the penetrance of this alteration was enhanced in the compound mutant (60–80% mice; Fig. 3K,L). Thus, although the hyperplastic lens epithelia phenotype of *Ring1*-deficient mice was not affected by a reduction of the dosage of *YY1*, the penetrance of the adherence of cornea and lens was increased. The results further strengthen the evidence for a genetic interaction between *YY1* and *Ring1*.

### 2.4. Complexes containing YY1 and class II PcG proteins

A possibility to explain this genetic interaction would be that YY1 and Ring1 belong to a common biochemical entity. However, using both yeast two-hybrid assays or in vitro pull down experiments we (unpublished results) and others (Satijn et al., 2001) have been unable to detect a direct interaction between YY1 and Ring1 or other class II PcG proteins. It could be that these proteins associate in complexes through interactions with other components of the complexes. To test this possibility, we introduced in tissue culture cells a plasmid that expresses a Myc-tagged YY1 protein together with plasmids in which cDNAs encoding class II PcG proteins were fused to the *E. coli* glutathione-*S*-transferase (GST) cDNA. In this way, protein complexes containing these GST-tagged proteins can be isolated by means of glutathione (GSH)-Sepharose beads Fig. 4). The results of this analysis showed that YY1 was co-isolated with GST-Ring1, GST-Rnf2 or GST-Bmi1 proteins (Fig. 4A, lanes 1–3) and that the formation of these complexes was independent of the GST moiety because no Myc-YY1 was bound to GSH-beads in extracts prepared from cells transfected with a plasmid, which expressed GST only (Fig. 4A, lane 4) or a non-PcG GST fusion protein (GST-CSF, Fig. 4A, lane 5). Deletional analysis showed that the association of YY1 into these complexes requires regions in both its N- and C-terminal moieties, since their truncation

Fig. 3. Anterior eye alterations in *Ring1* and *YY1*, *Ring1* compound mutant mice. Histological comparison of eye sections stained with hematoxylin and eosin from wild type and *YY1*$^{+/-}$ *Ring1*$^{-/-}$ newborn mice and embryos. Nasal is to the left, temporal to the right. Magnified views correspond to regions boxed in the panels immediately on top. Newborn mice (A–D). Wild type mice with a well formed anterior chamber (A,C). Mutant mice showing a deformed lens and no anterior chamber due to the adherence of the lens epithelium to the cornea (B,D). 17.5 dpc embryos (E,H). Wild type embryos with anterior chamber and a one-layer lens epithelium (E,G). Mutant embryos showing a corneolenticular adhesion and a hyperplastic lens epithelium (F,H). 15.5 dpc embryos (I,L). The anterior chamber is already formed in wild type embryos (I,K) but in mutant embryos there are contacts between the presumptive cornea and the lens. Abbreviations: nb, newborn; AC, anterior chamber; CS, corneal stroma; CEn, corneal endothelium; LE, lens epithelium; L, lens. Magnification ×10 (A,B), ×13.6 (E,F), ×15 (I,J), ×100 (C,D,G,H,K,L).

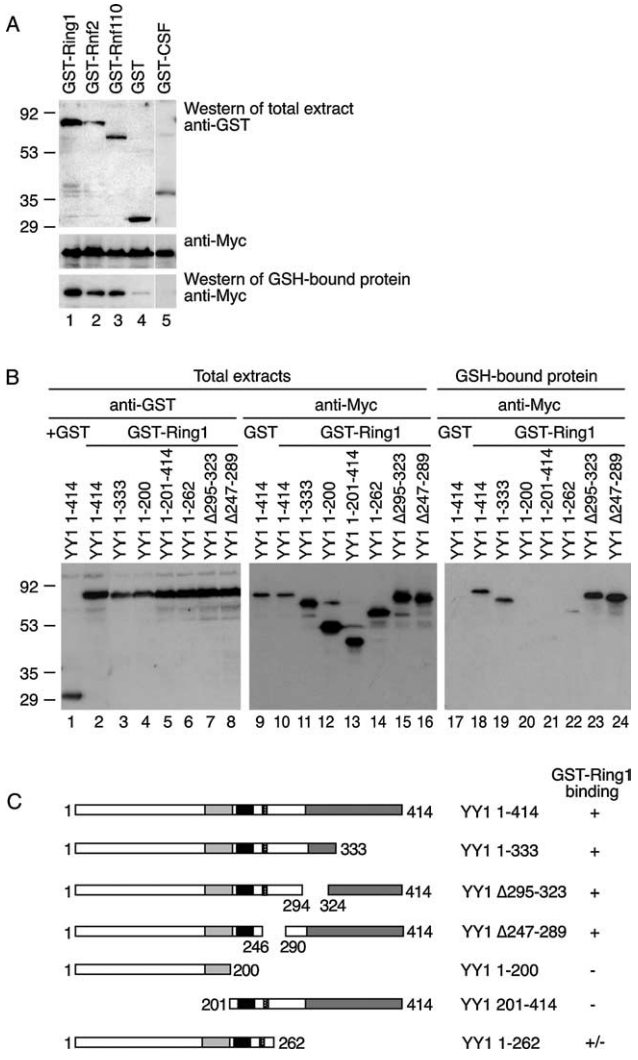


Fig. 4. Association of YY1 and class II PcG proteins. (A) Human kidney 293T cells were cotransfected with a plasmid expressing Myc-tagged YY1 and plasmids expressing GST alone or GST fused to the indicated proteins. Total extracts were probed by western blot with monoclonal anti-Myc antibody 9E10 or with anti-GST antibodies. Protein in cell extracts from transfected cells bound to GST beads were detected with the anti-Myc antibody. (B) Cells were transfected with Myc-tagged YY1 or the indicated truncated variants, together with a plasmid that expresses a GST-Ring1 fusion protein. The presence of transfected proteins was tested by western blot of total cell extracts using anti-Myc or anti-GST antibodies. The material in the cells extracts bound to GST beads was detected using a anti-Myc antibody. Sizes of molecular weight markers (in kilodaltan) are indicated on the left. (C) Diagram of intact and truncated YY1 proteins and summary of binding data. The boxes represent sequences conserved between mammalian and fly proteins corresponding to the following domains: clear grey, the histone deacetylase binding region; black, the EZH1/PC/PH binding region; stippled box, the CtBP1 binding motif; dark grey box, the DNA binding domain. The interaction between each YY1 protein and GST-Ring1 is designated by +, while $^{+/-}$ and − indicates very week or no interaction, respectively.

results in proteins [YY1(1–200), YY1(201–414)] that do not bind (Fig. 4B, lanes 20 and 21) or bind inefficiently [YY1(1–262), Fig. 4B, lane 22). A construct, which expressed a YY1 protein in which the three C-terminal zinc-fingers were deleted was efficiently bound to GSH-beads (Fig. 4B, lane 19). However, neither the deletion of only the first Zn finger (YY1 Δ295–323) nor of sequences before it (YY1 Δ247–289) affected the association of YY1 to the complex (Fig. 4B, lanes 23 and 24). Together, the data show that complexes containing YY1 and class II PcG proteins can form, and that the association of YY1 to this complex(es) relies at least in part on sequences conserved between mammalian and fly proteins.

## 3. Discussion

YY1 is an ubiquitiously expressed DNA binding protein with both transcriptionally activating and repressing activities (Thomas and Seto, 1999). YY1 also functions as a PcG protein, although evidence for this has been obtained mostly from work in *Drosophila* (Atchison et al., 2003). In the present study, we described homeotic alterations of the axial skeleton of newborn *YY1*$^{+/-}$ mice. Although homeotic phenotypes are not exclusive of PcG genes, they are usually found in PcG mutant mice. In addition, we also provide evidence for genetic interaction between *YY1* and a class II PcG gene, *Ring1*. Taken together, the results are consistent with a PcG function for the *YY1* gene in mammals.

Another common phenotype in PcG mutant mice, the (limited) anteriorization of rostral boundaries of Hox gene expression at the maintenance phase of their expression (Akasaka et al., 1996; Van der Lugt et al., 1996; Takihara et al., 1997), was not found in *YY1*$^{+/-}$ embryos. At earlier stages, 8.5 dpc of development, we did not found alterations either, which, at least for the subset of Hox genes analyzed, suggest that in this case the possibility of early, often transient, alterations of Hox gene expression patterns, which the genetic analysis shows it can have an impact on the formation of skeletal structures (Zakany et al., 1997; Bel-Vialar et al., 2000; Juan and Ruddle, 2003), cannot be considered here. A possible explanation is that, despite the homeotic phenotypes, the presence of YY1 in mutant embryos, although at lower levels than in wild type embryos, results in Hox gene mRNA alterations too subtle to be identified by whole mount in situ hybridization. In addition, there are examples of mouse embryos deficient in the product of some PcG genes, such as *Cbx2/M33* (Coré et al., 1997) or *Ring1* (del Mar Lorente et al., 2000), in which Hox gene expression is hardly altered, particularly in the mesodermal compartment, which will give raise to the axial skeleton. This is usually explained by gene redundancy, the situation in which the lack of a gene product is compensated by that of the products of its paralog(s). Recently, YY2, a homolog of YY1 that shares regions of homology identical to those conserved in *Drosophila* pho and phol has been described (Nguyen et al., 2004), which may also be functionally homologous. In contrast, using an in vitro differentiation system we have shown upregulation of Hoxb1 mRNA in embryoid bodies derived from *YY1*$^{+/-}$ ES cells, which is an indication that Hox genes can be regulated by YY1, and it is consistent with the unability of YY2 to compensate for YY1 deficiency in very early development (Donohoe et al., 1999). Additionally, the recent finding of the direct association of YY1 to some Hox proteins (Shi et al., submitted) suggests that alterations in Hox gene activities may take place in

*YY1*$^{+/-}$ embryos without involving a transcriptional control that might be reflected in Hox gene expression alterations. This illustrates the cross-regulatory interactions that may underlie the complex phenotypes observed in PcG mutants. Thus, whereas the nature of the homeotic transformations observed in these mutants is often posterior, there are examples in flies and in mammals of bidirectional transformations [*Pc*, *Cbx2*/*M33*, (Sato and Denell, 1985; Coré et al., 1997)] or, as it is the case for *YY1*, just anterior transformations [*Ring1*, (del Mar Lorente et al., 2000)]. Moreover, in some cases, for example, compound *Bmi1 Mel18* mutants (Akasaka et al., 2001), the correlation between posterior transformation phenotypes of PcG mutants and ectopic expression of Hox genes is not always found. Therefore, anterior transformations of the axial skeleton do not preclude the assignment into the PcG gene category.

Homeotic phenotypes were among the first ones identified in PcG mutant mice. Soon it was realized that other processes were affected, like the cerebellum maturation or hematopoietic differentiation (van der Lugt et al., 1994). Here, we describe a contribution of PcG genes to the development of the anterior segment of the eye. One of the key steps in the formation of the anterior chamber is the formation of a corneal endothelium, which is concurrent with the separation of the corneal mesenchyme from the lens (Cvekl and Tamm, 2004). Thus, in a number of mouse mutants involving transcription factors like Mf1/Foxc1 (Kidson et al., 1999) or signalling molecules such as TGFa, TGFb1 (Reneker et al., 2000; Flugel-Koch et al., 2002) the corneal endothelium fails to develop and the lens remains attached to the posterior side of the cornea. However, although our study lacks the ultrastructural analysis needed for a detailed citological definition of these structures, it seems that *Ring1*$^{-/-}$ and *YY1*$^{+/-}$ *Ring1*$^{-/-}$ mice lacking an anterior chamber, do have a corneal endothelium. This is consistent with the observation of identical Mf1/Foxc1 expression patterns in *YY1*$^{+/-}$ *Ring1*$^{-/-}$ and wild type littermate fetuses (data not shown). Since, the lens epithelia was also signalling, it is possible that other alterations occurred too, thus contributing to a defective separation from the cornea. One of the transcription factors expressed in the developing lens whose mutation results in a reduction of anterior chamber and adhesions between lens and corneal endothelium is Pax6 (Collinson et al., 2001). However, its expression was not noticeably affected in *YY1*$^{+/-}$ *Ring1*$^{-/-}$ mutants (data not shown). Thus, the molecular basis of the defects seen in *YY1*$^{+/-}$ *Ring1*$^{-/-}$ anterior eye remains to be determined.

The genetic interaction between *YY1* and *Ring1* is complex. Thus, whereas some phenotypes, such as the absence of a lens chamber, are enhanced in the compound mutant mice other, like some skeletal alterations, are decreased. Moreover, some homeotic transformations, or the lens epithelia defect, are similar in compound and single mutant mice. Our results contrast with the synergistic interactions observed for other murine PcG genes. For example, *Bmi1* and *Cbx2*/*M33*, two non-homologous class II PcG genes whose products are found in the same complex (Levine et al., 2002), show a synergistic interaction as indicated by homeotic transformations of compound mutants not seen in single mutants (Bel et al., 1998). However, this is the case mostly for the double homozygous mutation, which for *YY1* and *Ring1* cannot be generated due to the letality of the *YY1*$^{-/-}$ allele (Donohoe et al., 1999). In the case of *Bmi1* and *Mel18*, a strong interaction is observed in both *Bmi1*$^{+/-}$*Mel18*$^{-/-}$ and *Bmi1*$^{-/-}$*Mel18*$^{+/-}$ fetuses (Akasaka et al., 2001). However, the fact that *Bmi1* and *Mel18* are paralog genes is likely to reduce compensatory effects due to redundancy and, therefore, lead to a strong phenotype. Thus, it seems likely that *YY1* and *Ring1* participate together in the regulation of at least a subset of the gene targets involved in axial skeleton formation and anterior eye morphogenesis. Alternatively, it is possible that dosage sensitivity and functional redundancy for each of the two genes is different in the various regulatory pathways involved.

The molecular basis for the genetic interaction between *YY1* and the class II PcG gene *Ring1* is not known. Considering that both genes may potentially affect the expression of a large number of targets, the mechanistic link between *YY1* and *Ring1* could be an indirect one. However, our results show that despite the lack of evidence for a direct association between YY1 and Ring1, the two proteins are found in a heteromeric complex detected in extracts from transfected tissue culture cells. Similar complexes were also observed in cells transfected with only *YY1* or only *Ring1* expressing plasmids, but not in extracts prepared from not transfected cells (data not shown). Quite often, the complexes formed when the concentration of one or more of its components is artificially increased, like in cell transfectants, are thought to be artefactual and not a representation of the complexes found in more physiological conditions. However, there are examples of proteins for which functional and genetic interaction has been demonstrated and yet their biochemical detection in a defined complex has been unsuccessful. One such case is the interaction between the glucocorticoid receptor and HMBG1, whose association on chromatin has only recently been shown by biophysical (photobleaching FRET) methods (Agresti et al., 2005). It is worth noting the conspicuous absence of YY1 in most protein complexes isolated, including PcG complexes, despite its direct association to the products of the eed and EZH2 of the class I PcG genes (Satijn et al., 2001; Wang et al., 2004a), to the class II PcG fly proteins PC and PH (Mohd-Sarip et al., 2002) or to the Ring1 and YY1 binding protein RYBP (Garcia et al., 1999). While the reason for the unstability of the association of YY1 to these partners is unclear, our data suggest that some YY1 functions can occur through complexes containing class II PcG components such as a the Ring1/Rnf2 and Bmi1 proteins. This is consistent with the recent observation that pho recruiting to PREs in *Drosophila* needs of a Polycomb core complex that in addition to PC and PH contains PSC and SCE, the homologs of Bmi1 and Ring1, respectively (Mohd-Sarip et al., 2005).

## 4. Experimental procedures

### 4.1. Mice and genotyping

The generation of *Ring1* and *YY1* null mutant mouse lines, and the genotyping of the various alleles by Southern blot and PCR have been described (Donohoe et al., 1999; del Mar Lorente et al., 2000). *YY1*$^{+/-}$ mice were of a mixed 129, C57Bl6 genetic background, whereas *Ring1* mutant mice were of a mixed 129, Balb/c genetic background.

### 4.2. Skeletal preparations

Carcasses of newborn mice were skinned, eviscerated and fixed in 95% ethanol. The cartilage was stained with 0.2 mg/ml Alcian Blue (Sigma) in 75% ethanol/25% acetic acid overnight. After clearing in 2% KOH, the bone was stained with 0.075 mg/ml Alizarin Red in 1% KOH for 2 days.

### 4.3. RNA in situ hybridization and histology

Pregnant females were killed at the chosen gestation time. Noon on the day of the vaginal plug was taken as 0.5 day post coitum (dpc). For histological analysis, whole heads were fixed in 10% buffered formalin during 24 h. After dehydration and paraffin wax embedding, 3 μm sections were prepared and stained with hematoxylin and eosin following standard procedures. For in situ hybridization to mRNA, digoxigenin-labelled probes were hybridized to whole mount embryos (del Mar Lorente et al., 2000) or to cryostat sections of mouse embryos (Henrique et al., 1995) as described.

### 4.4. In vivo GST pull down assays

For expression of GST or GST-Ring1, GST-Bmi1 and GST-CSF proteins, the pEBG plasmid, which provides the *E. coli* glutathione-*S*-transferase (GST) at the N-terminus of the fusion proteins was used. A human *YY1* cDNA and truncated derivatives were subcloned into a pCS2Myc plasmid, which encodes six copies of a Myc tag (Rupp et al., 1994). Human embryo kidney 293T cells ($1.8\times10^6$ cells per 6 cm dish) received 2 μg of plasmid DNA (1 μg each of pCS2 and pEBG plasmids) complexed with FuGene (Roche). Cells were scraped from plates 40 h after transfection and total cell extracts were prepared as previously described (Garcia et al., 1999). Aliquots of cell extracts were mixed with 20 μl of GSH-Sepharose (50% packed volume, Sigma) previously incubated with 1% bovine serum albumin. After incubation for 1 h at 4 °C with continuous rotation, the beads were washed in lysis buffer, and bound proteins eluted, separated by SDS-PAGE and transferred to nitrocellulose filters for Western blot. The 9E10 mouse monoclonal anti-Myc antibody and rabbit IgG anti-GST antibodies bound to filters were visualized by chemiluminiscence (Amersham) using goat IgG anti-mouse IgG (Dako) or anti-rabbit IgG antibodies (BioRad) coupled to horseradish peroxidase, respectively.

### 4.5. In vitro differentiation of ES cells and RT-PCR

Embryonic stem (ES) cells were derived using standard techniques from *YY1*$^{+/-}$ intercrosses in an attempt to generate an isogenic series of alleles (Donohoe, unpublished data). The ES cells analyzed were derived from a set of blastocyst littermates. RNA was isolated from ES cells at day 0 (d0) of differentiation into embryoid bodies, d3 and d6 using TRIzol Reagent (Invitrogen). One microgram of total RNA was treated with RNAse-free DNAse, reverse transcribed with oligo dT, and triplicate reactions of 200 ng cDNA were amplified in SYBERGreen (BioRad) using the Bio-Rad iCycler iQ real-time PCR detection system (Bio-Rad). Relative mRNA abundance normalized to b-actin RNA levels was determined using the ΔΔ Ct method. The following set of primers were used: Hoxb1, forward 5′-AGGGCTGCCTAGCTCAGCGC and reverse 5′-AGCGTTGGAAGCC CAGTTAC; b-actin, forward 5′-GCCCCAGAGCAAGAGAGGTATCC and reverse 5′-ACGCACGATTTCCCTCTCAGC.

## Acknowledgements

We thank Dr Deschamps, M. Djabali, D. Duboule, B. Hogan, P. Gruss and R. Krumlauf, for providing Hox and other probes for in situ hybridization analysis. We are grateful to C. Calés and H. Koseki for critical reading of the manuscript. This work was supported by grants SAF2001-2211-CO2-01 and SAF2004-06952-CO2-01 (M.V.) from the DGI, Spanish Ministry of Science and Education and by NIH grant GM53874 (Y.S.). M.L. and C.S. were supported by fellowships from the Comunidad Autónoma de Madrid.

## References

Agresti, A., Scaffidi, P., Riva, A., Caiolfa, V.R., Bianchi, M.E., 2005. GR and HMGB1 interact only within chromatin and influence each other's residence time. Mol. Cell 18, 109–121.

Akasaka, T., Kanno, M., Balling, R., Mieza, M.A., Taniguchi, M., Koseki, H., 1996. A role for mel-18, a Polycomb group-related vertebrate gene, during the anteroposterior specification of the axial skeleton. Development 122, 1513–1522.

Akasaka, T., van Lohuizen, M., van der Lugt, N., Mizutani-Koseki, Y., Kanno, M., Taniguchi, M., et al., 2001. Mice doubly deficient for the Polycomb group genes Mel18 and Bmi1 reveal synergy and requirement for maintenance but not initiation of Hox gene expression. Development 128, 1587–1597.

Americo, J., Whiteley, M., Brown, J.L., Fujioka, M., Jaynes, J.B., Kassis, J.A., 2002. A complex array of DNA-binding proteins required for pairing-sensitive silencing by a polycomb group response element from the *Drosophila* engrailed gene. Genetics 160, 1561–1571.

Atchison, L., Ghias, A., Wilkinson, F., Bonini, N., Atchison, M.L., 2003. Transcription factor YY1 functions as a PcG protein in vivo. Eur. Mol. Biol. Org. J. 22, 1347–1358.

Bel, S., Core, N., Djabali, M., Kieboom, K., Van der Lugt, N., Alkema, M.J., et al., 1998. Genetic interactions and dosage effects of Polycomb group genes in mice. Development 125, 3543–3551.

Bel-Vialar, S., Core, N., Terranova, R., Goudot, V., Boned, A., Djabali, M., 2000. Altered retinoic acid sensitivity and temporal expression of Hox genes in polycomb-M33-deficient mice. Dev. Biol. 224, 238–249.

Brock, H.W., Fisher, C.L., 2005. Maintenance of gene expression patterns. Dev. Dyn. 232, 633–655.

Brown, J.L., Mucci, D., Whiteley, M., Dirksen, M.L., Kassis, J.A., 1998. The *Drosophila* Polycomb group gene pleiohomeotic encodes a DNA binding protein with homology to the transcription factor YY1. Mol. Cell 1, 1057–1064.

Brown, J.L., Fritsch, C., Mueller, J., Kassis, J.A., 2003. The *Drosophila* pho-like gene encodes a YY1-related DNA binding protein that is redundant with pleiohomeotic in homeotic gene silencing. Development 130, 285–294.

Cao, R., Wang, L., Wang, H., Xia, L., Erdjument-Bromage, H., Tempst, P., et al., 2002. Role of histone H3 lysine 27 methylation in Polycomb-group silencing. Science 298, 1039–1043.

Caretti, G., Di Padova, M., Micales, B., Lyons, G.E., Sartorelli, V., 2004. The Polycomb Ezh2 methyltransferase regulates muscle gene expression and skeletal muscle differentiation. Genes Dev. 18, 2627–2638.

Collinson, J.M., Quinn, J.C., Buchanan, M.A., Kaufman, M.H., Wedden, S.E., West, J.D., et al., 2001. Primary defects in the lens underlie complex anterior segment abnormalities of the Pax6 heterozygous eye. Proc. Natl Acad. Sci. USA 98, 9688–9693.

Coré, N., Bel, S., Gaunt, S.J., Aurrand-Lions, M., Pearce, J., Fisher, A., et al., 1997. Altered cellular proliferation and mesoderm patterning in Polycomb-M33-deficient mice. Development 12, 721–729.

Cvekl, A., Tamm, E.R., 2004. Anterior eye development and ocular mesenchyme: new insights from mouse models and human diseases. Bioessays 26, 374–386.

Czermin, B., Melfi, R., McCabe, D., Seitz, V., Imhof, A., Pirrotta, V., 2002. *Drosophila* enhancer of Zeste/ESC complexes have a histone H3 methyltransferase activity that marks chromosomal Polycomb sites. Cell 111, 185–196.

Dejardin, J., Rappailles, A., Cuvier, O., Grimaud, C., Decoville, M., Locker, D., et al., 2005. Recruitment of *Drosophila* Polycomb group proteins to chromatin by DSP1. Nature 434, 533–538.

del Mar Lorente, M., Marcos-Gutierrez, C., Perez, C., Schoorlemmer, J., Ramirez, A., Magin, T., et al., 2000. Loss- and gain-of-function mutations show a polycomb group function for Ring1A in mice. Development 127, 5093–5100.

Donohoe, M.E., Zhang, X., McGinnis, L., Biggers, J., Li, E., Shi, Y., 1999. Targeted disruption of mouse Yin Yang 1 transcription factor results in peri-implantation lethality. Mol. Cell. Biol. 19, 7237–7244.

Flugel-Koch, C., Ohlmann, A., Piatigorsky, J., Tamm, E.R., 2002. Disruption of anterior segment development by TGF-beta1 overexpression in the eyes of transgenic mice. Dev. Dyn. 225, 111–125.

Garcia, E., Marcos-Gutierrez, C., del Mar Lorente, M., Moreno, J.C., Vidal, M., 1999. RYBP, a new repressor protein that interacts with components of the mammalian Polycomb complex, and with the transcription factor YY1. Eur. Mol. Biol. Org. J. 18, 3404–3418.

Henrique, D., Adam, J., Myat, A., Chitnis, A., Lewis, J., Ish-Horowicz, D., 1995. Expression of a delta homologue in prospective neurons in the chick. Nature 375, 787–790.

Horard, B., Tatout, C., Poux, S., Pirrotta, V., 2000. Structure of a polycomb response element and in vitro binding of polycomb group complexes containing GAGA factor. Mol. Cell. Biol. 20, 3187–3197.

Juan, A.H., Ruddle, F.H., 2003. Enhancer timing of Hox gene expression: deletion of the endogenous Hoxc8 early enhancer. Development 130, 4823–4834.

Kidson, S.H., Kume, T., Deng, K., Winfrey, V., Hogan, B.L., 1999. The forkhead/winged-helix gene, Mf1, is necessary for the normal development of the cornea and formation of the anterior chamber in the mouse eye. Dev. Biol. 211, 306–322.

Kuzmichev, A., Nishioka, K., Erdjument-Bromage, H., Tempst, P., Reinberg, D., 2002. Histone methyltransferase activity associated with a human multiprotein complex containing the enhancer of Zeste protein. Genes Dev. 16, 2893–2905.

Kwon, H.J., Chung, H.M., 2003. Yin Yang 1, a vertebrate polycomb group gene, regulates antero-posterior neural patterning. Biochem. Biophys. Res. Commun. 306, 1008–1013.

Lessard, J., Sauvageau, G., 2003. Polycomb group genes as epigenetic regulators of normal and leukemic hemopoiesis. Exp. Hematol. 31, 567–585.

Levine, S.S., Weiss, A., Erdjument-Bromage, H., Shao, Z., Tempst, P., Kingston, R.E., 2002. The core of the polycomb repressive complex is compositionally and functionally conserved in flies and humans. Mol. Cell. Biol. 22, 6070–6078.

Levine, S.S., King, I.F., Kingston, R.E., 2004. Division of labor in polycomb group repression. Trends Biochem. Sci. 29, 478–485.

Mohd-Sarip, A., Venturini, F., Chalkley, G.E., Verrijzer, C.P., 2002. Pleiohomeotic can link polycomb to DNA and mediate transcriptional repression. Mol. Cell. Biol. 22, 7473–7483.

Mohd-Sarip, A., Cleard, F., Mishra, R.K., Karch, F., Verrijzer, C.P., 2005. Synergistic recognition of an epigenetic DNA element by Pleiohomeotic and a Polycomb core complex. Genes Dev. 19, 1755–1760.

Muller, J., Hart, C.M., Francis, N.J., Vargas, M.L., Sengupta, A., Wild, B., et al., 2002. Histone methyltransferase activity of a *Drosophila* Polycomb group repressor complex. Cell 111, 197–208.

Nguyen, N., Zhang, X., Olashaw, N., Seto, E., 2004. Molecular cloning and functional characterization of the transcription factor YY2. J. Biol. Chem. 279, 25927–25934.

Ogawa, H., Ishiguro, K., Gaubatz, S., Livingston, D.M., Nakatani, Y., 2002. A complex with chromatin modifiers that occupies E2F- and Myc-responsive genes in G0 cells. Science 296, 1132–1136.

Otte, A.P., Kwaks, T.H., 2003. Gene repression by Polycomb group protein complexes: a distinct complex for every occasion? Curr. Opin. Genet. Dev. 13, 448–454.

Pirrotta, V., Gross, D.S., 2005. Epigenetic silencing mechanisms in budding yeast and fruit fly: different paths, same destinations. Cell 18, 395–398.

Reneker, L.W., Silversides, D.W., Xu, L., Overbeek, P.A., 2000. Formation of corneal endothelium is essential for anterior segment development—a transgenic mouse model of anterior segment dysgenesis. Development 127, 533–542.

Ringrose, L., Paro, R., 2004. Epigenetic regulation of cellular memory by the Polycomb and Trithorax group proteins. Annu. Rev. Genet. 38, 413–443.

Ringrose, L., Rehmsmeier, M., Dura, J.M., Paro, R., 2003. Genome-wide prediction of Polycomb/Trithorax response elements in *Drosophila* melanogaster. Dev. Cell 5, 759–771.

Rupp, R.A., Snider, L., Weintraub, H., 1994. Xenopus embryos regulate the nuclear localization of XMyoD. Genes Dev. 8, 1311–1323.

Satijn, D.P., Hamer, K.M., den Blaauwen, J., Otte, A.P., 2001. The polycomb group protein EED interacts with YY1, and both proteins induce neural tissue in *Xenopus* embryos. Mol. Cell. Biol. 21, 1360–1369.

Sato, T., Denell, R.E., 1985. Homoeosis in *Drosophila*: anterior and posterior transformations of Polycomb lethal embryos. Dev. Biol. 110, 53–64.

Shi, Y., Sawada, J., Sui, G., Affar, E.B., Whetstine, J.R., Lan, F., et al., 2003. Coordinated histone modifications mediated by a CtBP co-repressor complex. Nature 422, 735–738.

Srinivasan, L., Atchison, M.L., 2004. YY1 DNA binding and PcG recruitment requires CtBP. Genes Dev. 18, 2596–2601.

Takihara, Y., Tomotsune, D., Shirai, M., Katoh-Fukui, Y., Nishii, K., Motaleb, M.A., et al., 1997. Targeted disruption of the mouse homologue of the *Drosophila* polyhomeotic gene leads to altered anteroposterior patterning and neural crest defects. Development 124, 3673–3682.

Thomas, M.J., Seto, E., 1999. Unlocking the mechanisms of transcription factor YY1: are chromatin modifying enzymes the key? Gene 236, 197–208.

Valk-Lingbeek, M.E., Bruggeman, S.W., van Lohuizen, M., 2004. Stem cells and cancer; the polycomb connection. Cell 118, 409–418.

van der Lugt, N.M., Domen, J., Linders, K., van Roon, M., Robanus-Maandag, E., te Riele, H., et al., 1994. Posterior transformation, neurological abnormalities, and severe hematopoietic defects in mice with a targeted deletion of the bmi-1 proto-oncogene. Genes Dev. 8, 757–769.

Van der Lugt, N.M.T., Alkema, M., Berns, A., Deschamps, J., 1996. The polycomb-group homolog Bmi-1 is a regulator of murine Hox gene expression. Mech. Dev. 58, 153–164.

Wang, L., Brown, J.L., Cao, R., Zhang, Y., Kassis, J.A., Jones, R.S., 2004a. Hierarchical recruitment of Polycomb group silencing complexes. Cell 14, 637–646.

Wang, H., Wang, L., Erdjument-Bromage, H., Vidal, M., Tempst, P., Jones, R.S., et al., 2004b. Role of histone H2A ubiquitination in Polycomb silencing. Nature 431, 873–878.

Zakany, J., Gerard, M., Favier, B., Duboule, D., 1997. Deletion of a HoxD enhancer induces transcriptional heterochrony leading to transposition of the sacrum. Eur. Mol. Biol. Org. J. 16, 4393–4402.